MICROWAVE WAVEGUIDE MODULATORS FOR C02 LASERS

P. K. Cheo, et al

United Aircraft Research Laboratories

Prepared for:

Office of Naval Research
Advanced Research Projects Agency

25 September 1974

N921513-8

Fourth Semi-Annual Technical Report

Microwave Waveguide Modulators For CO_2 Lasers

by

P. K. Cheo, M. Gilden, D. Fradin and R.Wagner
United Aircraft Research Laboratories
East Hartford, Connecticut 06108

September 25, 1974

Principal Investigator: P. K. Cheo (203) 565-4297

Prepared for the Office of Naval Research
Contracting Officer: Dr. M. White
Contract No. N00014-73-C-0087
Contractor Modification No. P00002 - $313,780.00
25 August 1972 to 25 June 1975

Sponsored by
Advanced Research Projects Agency
ARPA Order 1860, Amendment No. 9/11-15/72

TABLE OF CONTENTS

1.0 TECHNICAL REPORT SUMMARY

1.1 Program Objectives

The long-range objective of this program is to develop an efficient and reliable ultra-wideband waveguide modulator for CO_2 lasers that will be useful for high-resolution, imaging optical radars and high-data-rate optical communication systems. The efficiency and reliability are obtainable by using integrated optics technology. Because this technology is still at an early stage of development many novel concepts must be demonstrated and techniques be developed. Of particular concern during the present program are several critical items which must be investigated in order to extablish a firm basis toward the development of infrared waveguide modulator. They are (1) the determination of attenuation constant, α, for grating couplers (2) the determination of the effects of thin metal-layers on coupling and propagation of optical beams as well as on microwaves, and (3) synchronization requirements and effects of dispersion of a traveling microwave in a mini-gap ridge waveguide section filled with one-mil GaAs slab. During the present reporting period (March 26 to September 26, 1974) efforts have been made to analyze these problems theoretically and experimentally.

1.2 Major Accomplishments

During this reporting period four significant advances in the modulator development have been made. The first two concerns with the structural quality of GaAs waveguides. The grating couplers which are an integral part of the waveguide structure are now being made by ion-beam milling technique instead of rf sputter-etching. This change of etching technique has provided remarkable improvement in the fabrication procedure. Preliminary results indicate that the grooves definition is now limited essentially by the mask pattern and the groove profile can be well controlled by using ion-beam milling technique. The second improvement involves the ruggedization of GaAs waveguide structure. The strength of a chemo-mechanically polished GaAs slab is very weak and has caused some difficulties during handling and processing cycles. For this and a number of other reasons which shall be discussed in later section of this report, we have developed a relatively strain-free metalization process by which thin ($\sim$ 20 μm) layers of nickel-copper are deposited on the surfaces of GaAs slab. The metallic layer has provided a considerable strength to the GaAs waveguide structure.

The next two significant accomplishments relate to the microwave aspects of the modulator development. With a traveling wave structures, we have demonstrated that the bandwidth of this modulator can be made in excess of 2 GHz at Ku band. This includes synchronization and impedance matching which were accomplished by using respectively a finite number of periodic discontinuities in the ridge section and

quarter wave transformers. One of the most significant result during this interm period is the experiment employing very high power to test the modulator. The result indicates that no failure is expected under a cw mode operation of this modulator at an input microwave power level in excess of 100 watts.

1.3 Future Work

Sideband power at Ku-band can be substantially increased from the results of our preliminary experiment (Ref. 1) by increasing the optical coupling and the modulator length. The physics of prism and grating couplers is now fairly well understood (Ref. 2). Work will be continued to improve the coupling efficiency and the transmitted optical beam quality. In the meantime the ruggedness, uniformity and reproducibility of the waveguide structure will be improved to permit the use of optimum length GaAs thin-slabs that can best meet the goal of this program.

In the near term this work will be directed toward the attainment of a modulator which will be capable of providing a frequency chirped CO_2 laser power in the range from 5 to 10 mW at frequencies about 16 GHz offset from the P(20) 00^01 - 10^00 vibrational-rotational transition. Such a modulator is useful (Ref. 3) for laboratory testing a number of radar system concepts.

The schedule for these tasks is shown in Table I.

TABLE I-Program Schedule For The Development
of Microwave Waveguide Modulators

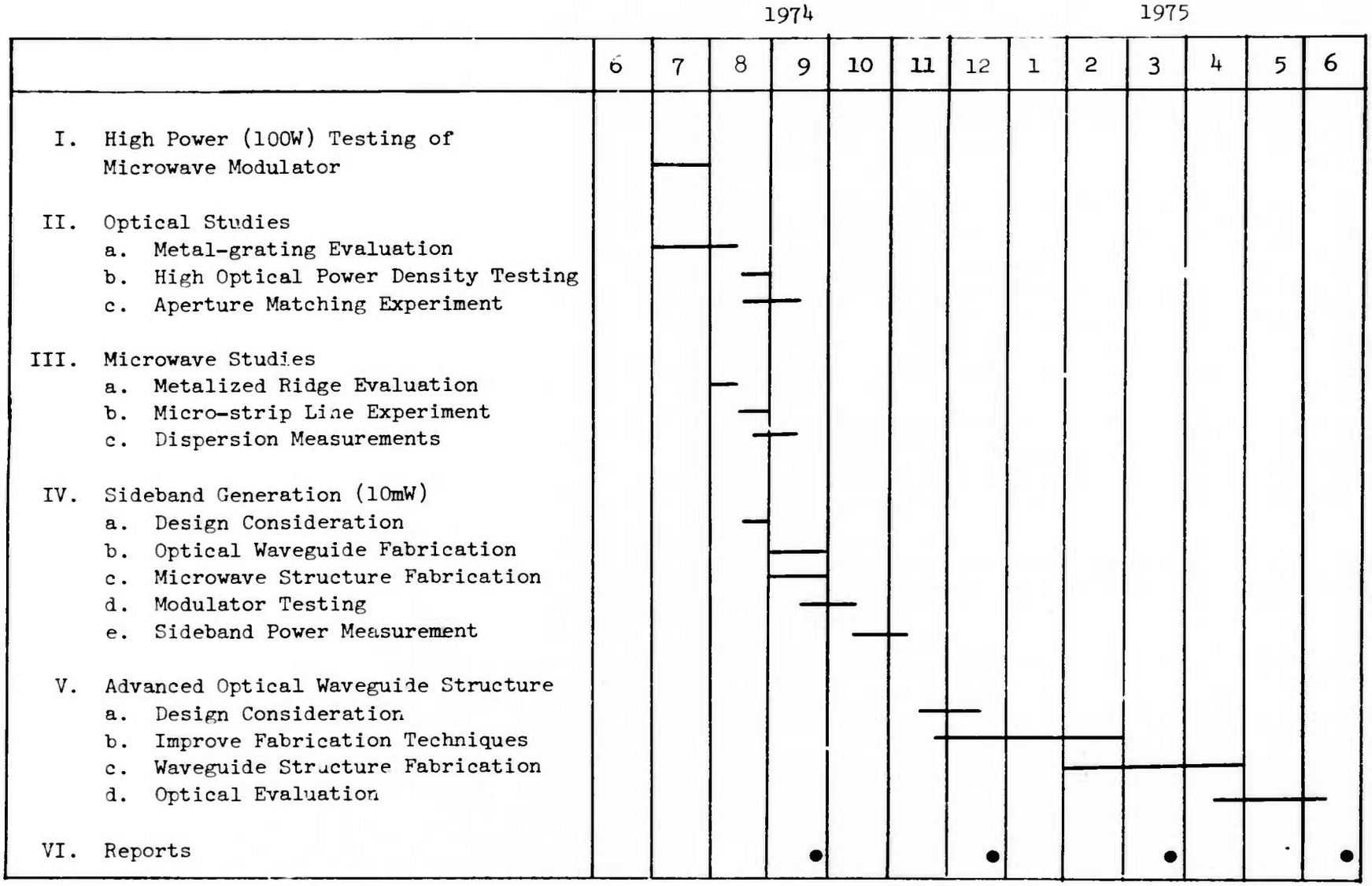

2.0 NEW WAVEGUIDE MODULATOR STRUCTURE

2.1 Introduction

The ir waveguide modulator is being developed under this program which utilizes both optical and microwave waveguide properties (Ref. 1,2), An ir waveguide modulator that can provide a bandwidth in excess of 2 GHz and can be operated in a cw mode at an input microwave power level in excess of 100 watts is reported. The phase shift modulation technique is identical to that presently being developed at Lincoln Laboratory (Ref. 3) with the exception that a GaAs thin-slab optical waveguide modulator is used instead of bulk crystals. A frequency chirped CO_2 laser waveform at frequencies ranging from 15 to 17 GHz offset from the CO_2 molecular laser resonance can be generated by a frequency modulation of the microwave driving signal which is properly synchronized and impedance-matched into the ridge-section of a mini-gap traveling-wave microwave transmission line.

Because of excessive microwave power attenuation in the n^+ substrate of the epitaxially grown GaAs thin film optical waveguide (Ref. 4), the decision has been made at this point in time to use the high resistivity GaAs thin-slab as the optical waveguide. It is made by a careful thinning of a large GaAs bulk wafer from a thickness of 0.015 inch down to about 0.001 inch. The use of the chemo-mechanically polished GaAs thin-slabs presents some difficulties in handling as well as in optical coupling. Sections 2.2 shall address these structural problems and present our techniques which have recently been developed for ruggedizing these structures and improving the optical coupling efficiency.

Another related problem which must be considered here is the mode characteristics of these waveguides. Optical coupling and propagation losses are strongly dependent on the mode structure of the guide. We have previously (Ref. 4) computed the β_m values for the TE modes of a chemo-mechanically thinned GaAs waveguide with index profile $n_0 = 1.0$, $n_1 = 3.275$ and $n_2 = 1.0$. This computation was made by using the formulation derived by Tien and Ulrich (Ref. 5) for semi-infinite planar waveguides using the zig-zag path model. In that model a guided wave mode is established as a result of total internal reflection at two boundaries when the total phase change in the direction normal to the waveguide is an integral multiple of π This expression is given by (Ref. 5)

$$d = \frac{1}{b_1} \left[m\pi + \tan^{-1}(\rho_0/b_1) + \tan^{-1}(\rho_2/b_1) \right] \qquad (1)$$

where d is the thickness of the waveguide and the indice m = 0, 1, 2, - - - -. Other

parameters are related by the set of equations:

$$b_1^2 = (kn_1)^2 - \beta_m^2$$

$$\rho_o^2 = \beta_m^2 - (kn_o)^2 \qquad (2)$$

$$\rho_2^2 = \beta_m^2 - (kn_2)^2$$

To be more cost-effective, GaAs has been employed exclusively as the optical waveguide material simply because this material is commercially available at relatively low cost and has good optical and electrical properties. At the present stage of development, this program consums a large amount of material. As fabrication techniques are further developed to minimize the possibility of unintentional loss of the modulator, more exotic and expensive materials such as CdTe and ZnSe may be used to replace GaAs. Figures 1-3 show the mode structures of three types of waveguides. Figure 1 and 2 give the mode dispersion curves, respectively, for a single layer GaAs and CdTe waveguides, and Fig. 3 gives the results for a heterostructure which consists of a CdTe waveguide coated with a layer of ZnSe thin film. From these results, it is clear that the mode discrimination is increasingly improved as the difference in refractive indices between the guided layer and the surrounding media is decreased. Better mode discrimination would enhence the modulator performance in the following ways: (1) It will be possible to minimize the propagation loss as a result of mode-conversion; (2) it will increase the probability of generating the lowest order guided wave mode, which has the lowest attenuation loss, expecially when a metal claded ridge waveguide structure is used, as discussed in Sections 2.2 and 4.0; and (3) it may be possible to improve the optical coupling efficiency by utilizing backward excitation through the ZnSe layer acting as a substrate (Ref. 6).

2.2 Fabrication and Processing

During this reporting period, effort has been made in the following three areas: (1) Ion milling of phase gratings, (2) Ion thinning of GaAs wafers, and (3) metallizing GaAs thin-slabs at or near room temperature in order to produce a low thermally strained thin film.

Prelinimary experiments with our recently installed ion milling facility indicate that high quality phase gratings with desired aspect ratio and groove profile

FIG. 1

TE MODES CHARACTERISTICS OF A SINGLE LAYER GaAs OPTICAL WAVEGUIDE

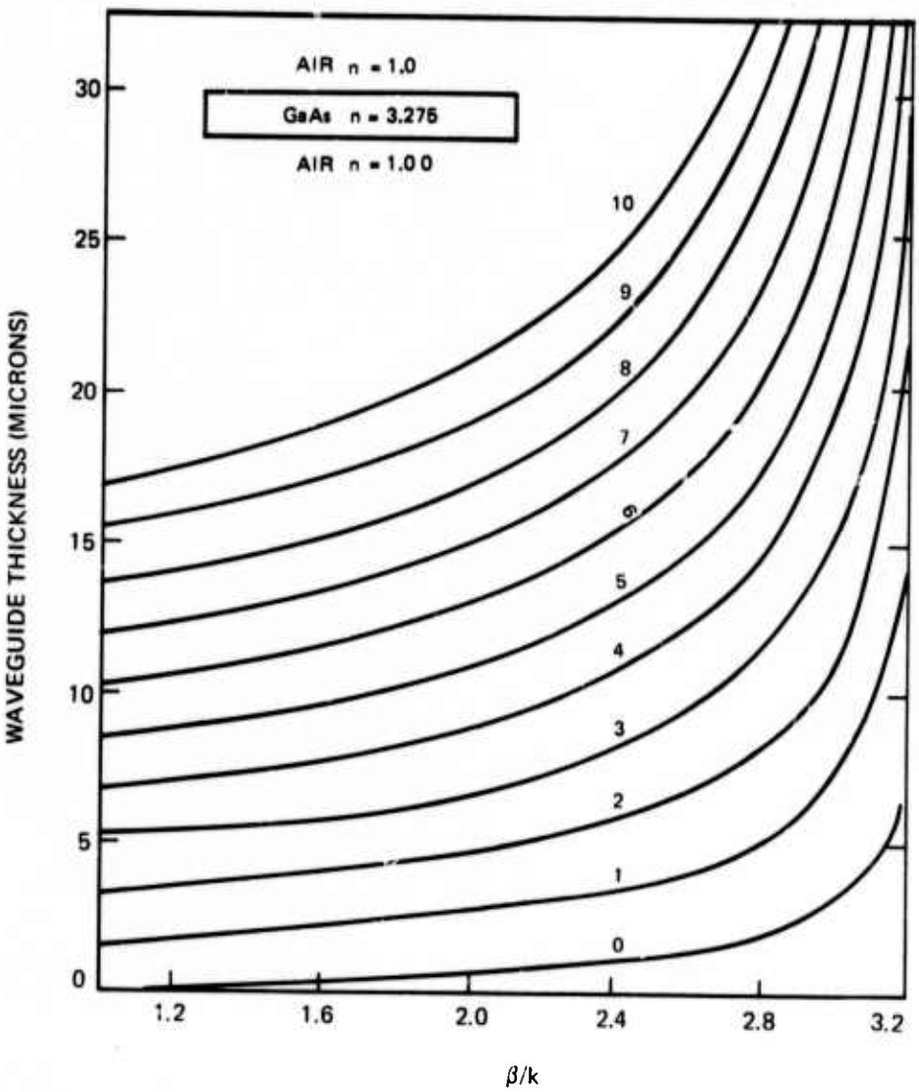

2.2a

FIG. 2

TE MODE CHARACTERISTICS OF A SINGLE LAYER CdTe OPTICAL WAVEGUIDE

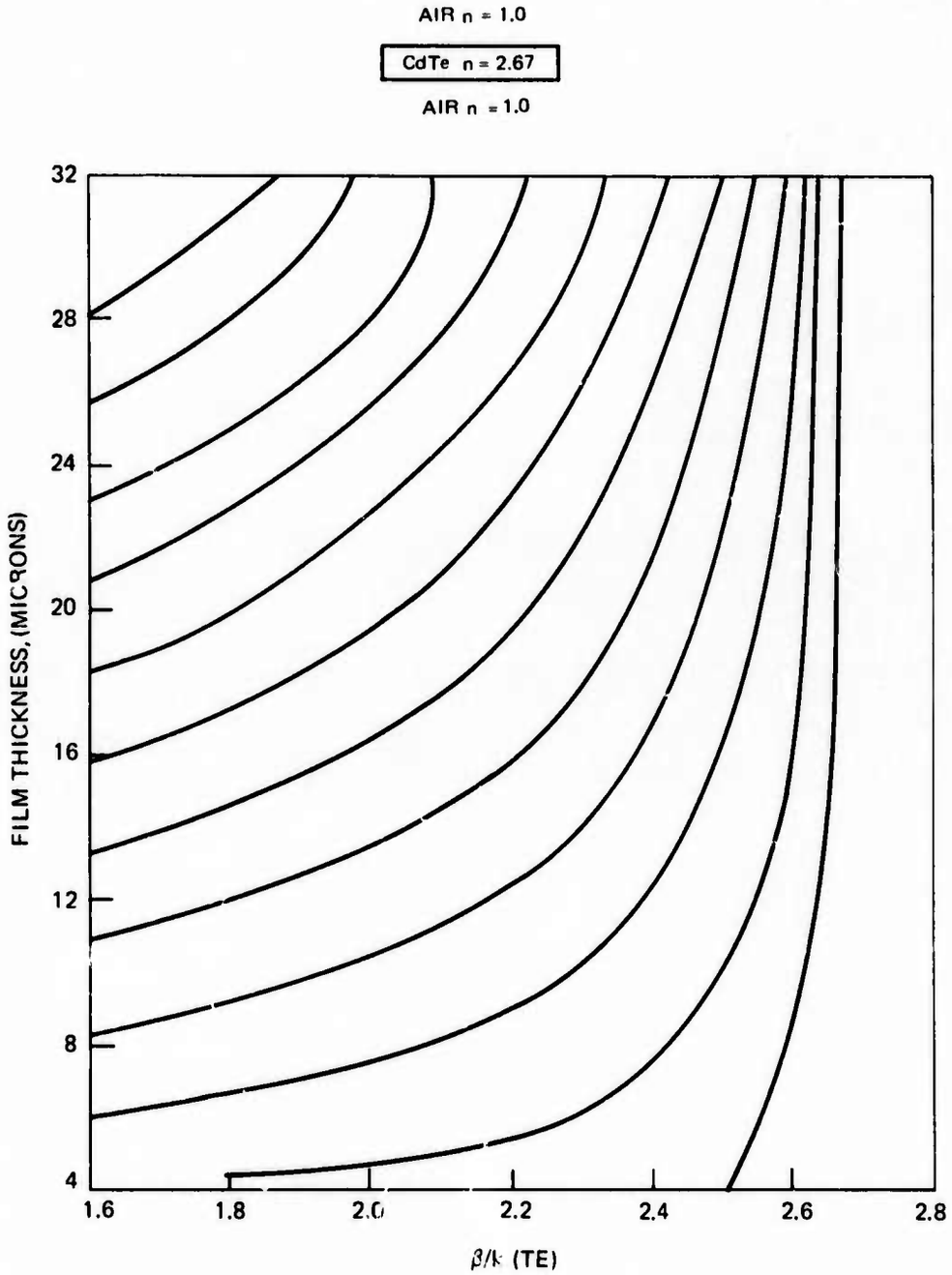

N09-124-1

TE MODE CHARACTERISTICS OF A MULTI–LAYER CdTe OPTICAL WAVEGUIDE

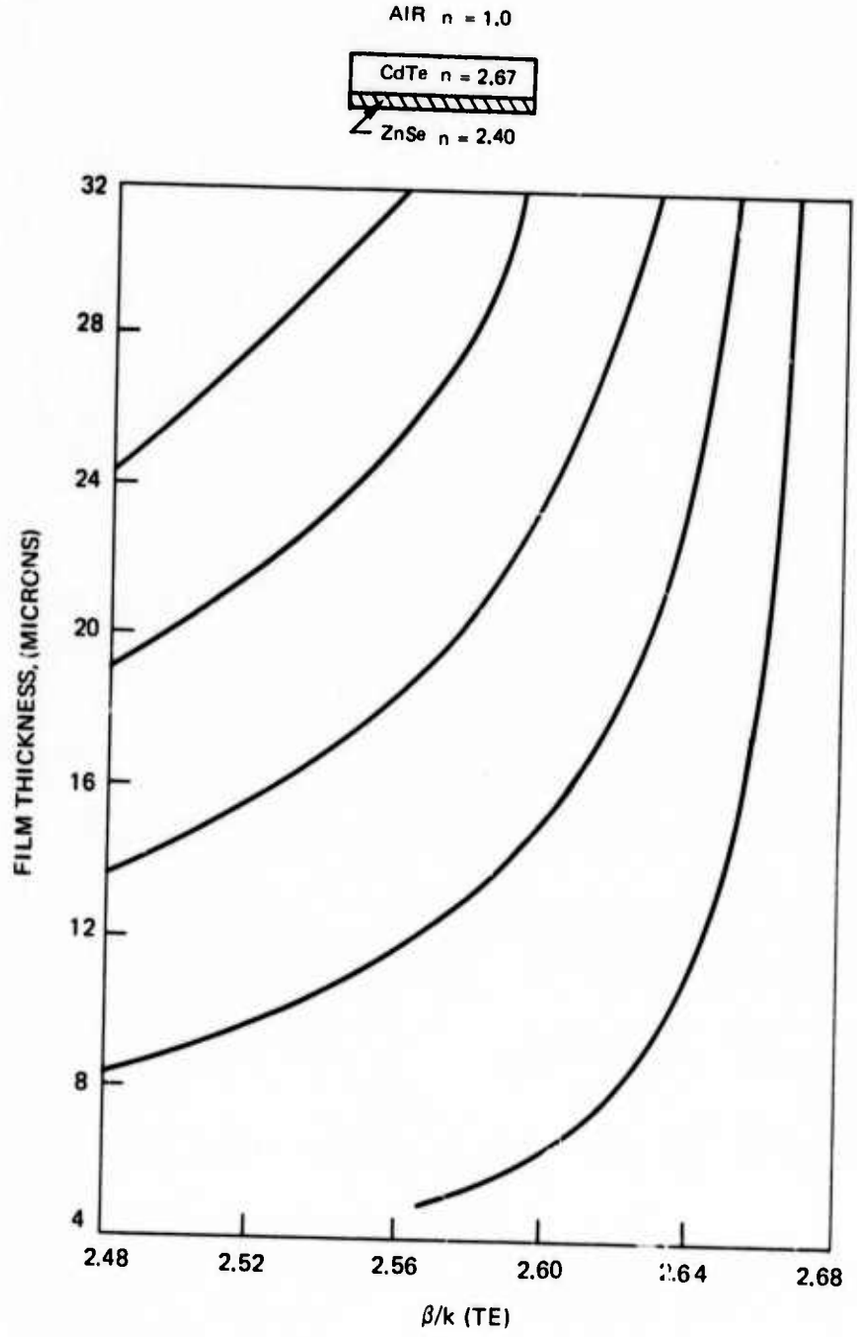

2-2c

can be obtained, and that uniform thinning and high specular finishing of large GaAs surfaces (2" x 2") can also be obtained.

Phase grating fabrication procedure can be summarized as follows:

1. Photoresist chemo-mechanically polished wafer.
2. Expose and develop required image. In this case a photomask having a 2.75 μm periodicity line spacing is used.
3. Post bake the resist in vacuum at 140°C.
4. Mount wafer on copper block with high vacuum grease.
5. Ion mill phase grating grooves into GaAs material.

Shipley 1350J photoresist having a thickness of one micron was used in the above sequence. Groove depths on the order of 1 μm have been achieved. Figure 4 displays a 1,000x profile of a wafer processed in the above sequence. The aspect ratio is fairly good. Noted that the side walls of the gratings are almost perpendicular; an indication of no undercutting. Aspect ratio was controlled by tailoring photomask aspect ratio as well as optimizing the parameters of the ion mill. A wide latitude of current densities are available with the ion mil (up to 1 ma/cm^2). Work is still in progress to develop techniques for producing gratings with a variety of groove profiles for future experiments. Figure 5 shows some of our recent phase gratings which are specially made to yield rectangular, sinusoidal and blazed groove profiles for future experiments.

Thinning of GaAs wafers by using ion milling proceeds at a rate of 4 μm/hour. This is an ideal means of thinning wafers to a 20 μm or less thickness, after the wafer has been chemo-mechanically polished to a thickness in the range of 25-30 μm. Experiments have been performed to determine this milling rate at which thinning of wafers can proceed while still maintaining a high specular finish. A higher thinning rate is possible (Ref. 7) by changing the angle of incidence of the impinging ion beam upon the substrate.

Efforts are being carried out to determine a means of metallizing GaAs which will yield low stress metal films. Metallized GaAs waveguides offer several advantages. It will increase the ruggedness of thin-slab optical devices for safe handling, and will also provide a good thermal conduction so that this modulator can be used in high power systems for which large heat dissipation capabilities are required.

Some of the requirements of a metallized film on GaAs are:

1. Good conductivity, electrical & thermal
2. Good adhesion between GaAs and the metallized film.
3. Minimum stresses between GaAs and the metal and of the metal itself
4. Thickness uniformity of the metallized film must be within 1 μm.

SCANNING ELECTRON MICROGRAPH OF A PHASE GRATING
WITH RECTANGULAR GROOVES

(5000X)

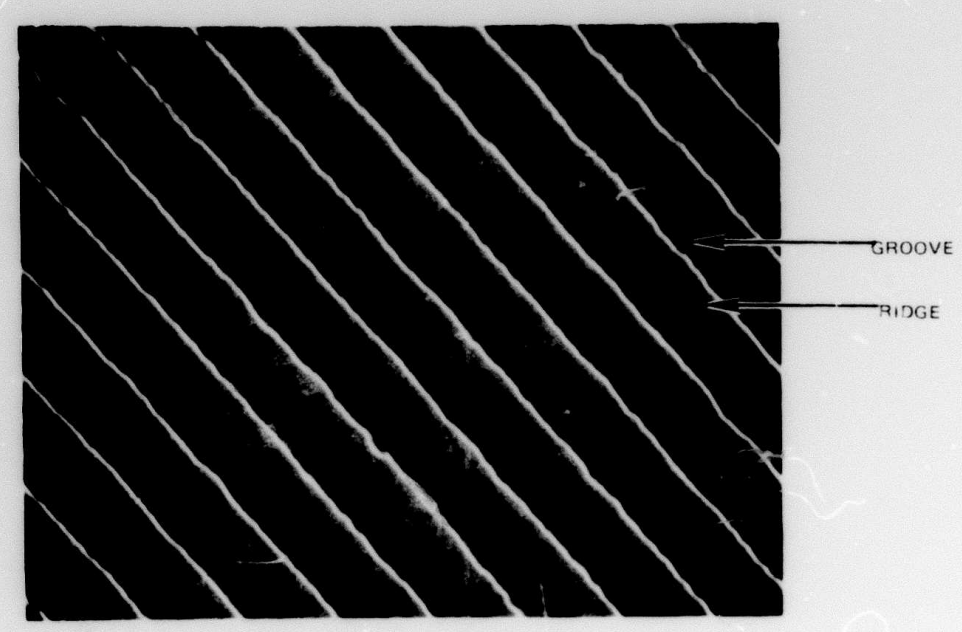

2-3a

PHASE GRATINGS OF VARIOUS GROOVE PROFILES IN GaAs THIN SLABS

(1000X)

a) RECTANGULAR GROOVES

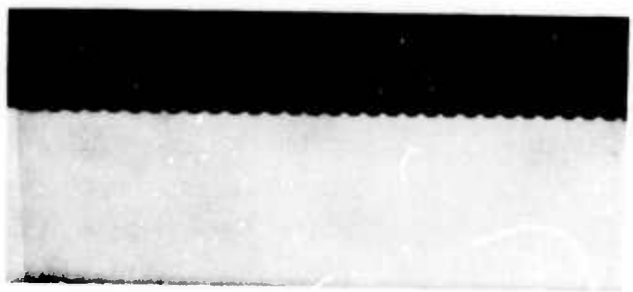

b) SINUSOIDAL GROOVES

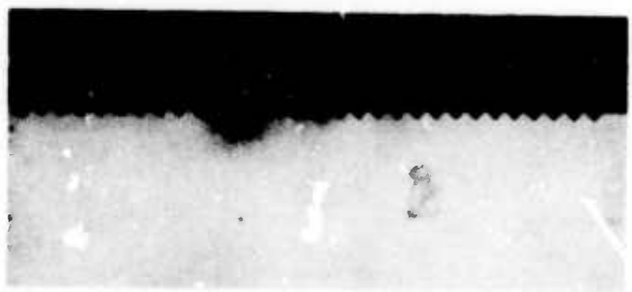

c) BLAZED GROOVES

Previous experiments (Ref. 4) indicated that the stresses of the metallized film were so high that wafer cleavage was almost always inevitable. In the case of rf sputtered metallic films, the temperatures incurred during rf sputtering process are probably the largest contributor to stresses in the metal. Electroplating on the other hand, also produced considerable stresses when the process was carried out at elevated temperatures (160°F-170°F). Other factors causing stresses in electroplated films are:

1. Current density
2. Anode to cathode ratio
3. Impurities in the electrolyte
4. Depth of filtration
5. Anealing

These parameters can be optimized to reduce the stresses formed in an as plated metal. In fact one can alter these parameters to change stresses from compression to tension (Ref. 8).

To circumvent the temperature effects of the above mentioned metallization requirements, a system of electroless/electrolytic metallization is presently being employed. This system works well at room temperature, and offers a means of applying metallic layers quickly and efficiently. While some stress is apparent with this system, no wafers have been lost due to cleavage as mentioned earlier. Basically the system consist of electrolessly depositing a thin film (.5 μm) of Nickel/Boron alloy onto a GaAs wafer, then subsequently electroplating over this film from a copper sulphate/sulphuric acid electroplating bath to the desired thickness (25 μm).

To initiate electroless plating on GaAs wafers its surface must first be sensitized. This is accomplished by "seeding" the surface with palladium chloride crystals from an aqueous solution containing palladium chloride and hydrochloric acid. The palladium chloride is then chemically reduced to form palladium on the GaAs surface which acts as a catalyst to initiate plating of the Nickel/Boron alloy. The electroless nickel bath is maintained at a constant temperature of 50°C.

The electroless nickel is then electroplated with copper at room temperature to a thickness of 25 μm. The copper electroplate used contains brighteners, and leveling agents to maintain thickness uniformity. Tally surf measurements on an electroplated wafer show that the uniformity of the resultant metal film can be maintained to within ± 1 μm over 4.5 cm^2 area.

Experiments are now underway to determine precisely to what extent that metallized films will have on optical coupling. It is believed that by metallizing the grating side of a GaAs thin-slab waveguide, the strength of coupling will increase as a result of redistribution of optical power particularly from the forward to the waveguide direction. Figure 6 displays a GaAs wafer with metallization, under the

FIG. 6

COMPOSITE GaAs WAVEGUIDE WITH A THICK Ni–Cu FILM

metallic film there are three optical grating couplers. These grating couplers were ion milled into the GaAs. The gratings can not be distinguished due to the thick (25 μm) layer of copper. Noted that the metallized wafer is slightly bowed. This shows the as-plated metal under stress which tends to pull away from the GaAs wafer. This tested sample was completely processed at out laboratory through the following sequence:

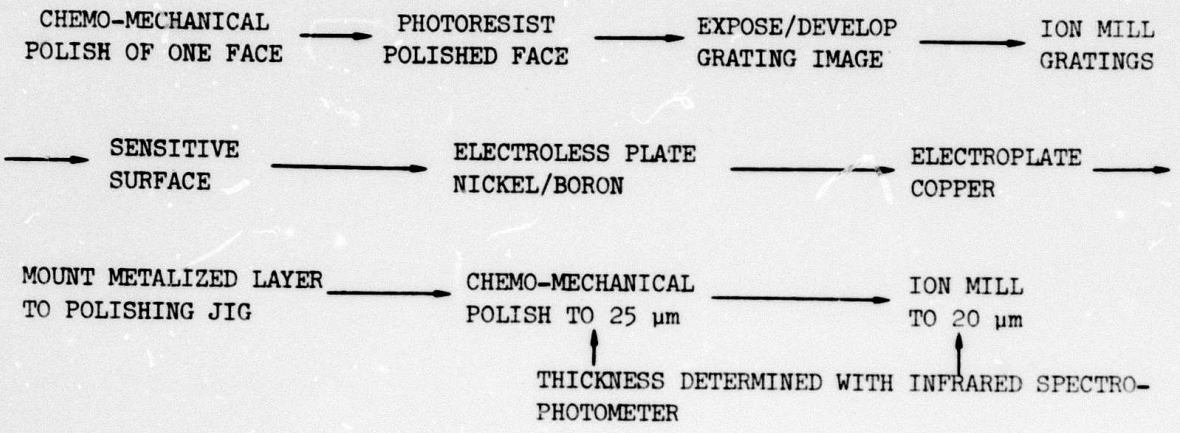

Efforts are under way to assay the quality of the copper films being produced. Figure 7 displays a 0.010 inch GaAs wafer with 0.001 inch of copper film deposited on the opposing faces. This configuration will be used to determine the quality of the copper film to be used as a microstrip waveguide. Work is still in progress to refine the metalizing technique. Of particular interest is the removal of remaining stresses in the as-plated metallic films and to improve the purity of copper.

Ion beam deposition of metals may prove to be an effective means of depositing low stress metals on GaAs (Ref. 7). This operation takes place in a high vacuum (5×10^{-5} TORR) and at relatively low temperatures ($60^{o}C$). This may be a favorable means of producing a thin conductive layer for subsequent electroplating.

In summary, ion milling has improved and simplified the technique for processing phase gratings in GaAs, and will be beneficial in thinning wafers to 20 μm or less. A system for metallizing GaAs wafers has been developed which yields a marked improvement over previous methods. Additional work is required to further improve the quality of optical waveguide modulator.

COMPOSITE GaAs WAVEGUIDE WITH METALLIC FILMS ON BOTH SURFACES

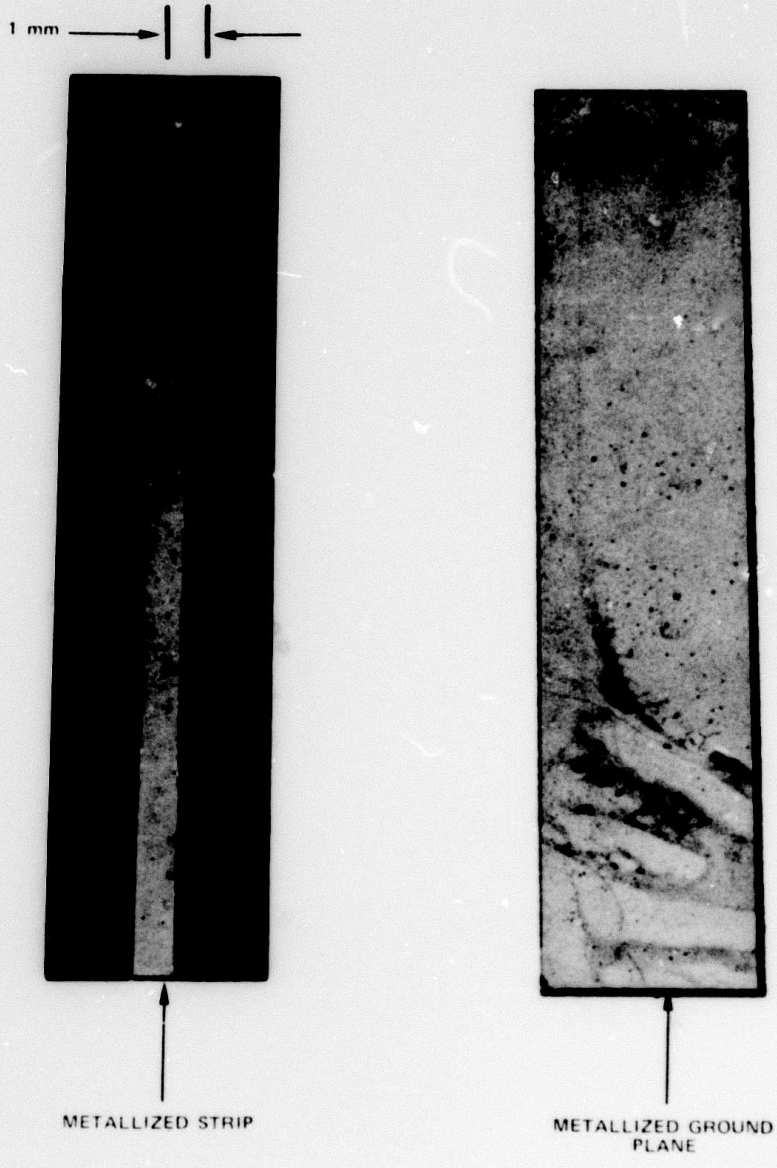

3.0 OPTICAL STUDIES OF WAVEGUIDE MODULATORS

3.1 Introduction

The useful optical power transmitted through most of our previously tested modulators is about 1 percent, whereas efficiencies of over 50 percent are theoretically possible for uniform grating pairs. As noted in the previous technical reports (Ref. 2 and 4), the low observed coupling efficiency may be the result of a number of factors that include multiple diffracted beams corresponding to the same diffracted order, mode conversion, and lack of proper aperture matching. An experimental investigation has now been initiated to determine and eliminate the causes of the unsatisfactory performance.

The experimental investigation consists of two parts. In the first part a systematic study of the optical characteristics of the symmetric waveguide modulator configuration is being conducted. From this study values of the leaky wave parameter α and the power transfer coefficients are being obtained and correlated with the grating geometry. Since these parameters vary with mode number, they are being measured for several guided modes. In addition, the extent of mode conversion within the waveguide is being determined by means of angular scans of the two out-coupled beams. Preliminary results obtained in this study are described below. These results were obtained with high-quality, chemically etched gratings and represent the best performance obtained to date. Total coupling efficiencies of about 7 percent have been measured. About half of this out-coupled energy can be retained as useful output.

During the second part of the experimental investigation, the optical properties of an asymmetric, metal-clad waveguide will be studied in detail and compared to the optical properties of the symmetric waveguide. The useful coupling obtained with the metal-clad waveguide should be significantly greater than that obtained with a symmetric waveguide, because the metal coating will both increase the value of α, thereby facilitating proper aperture matching, and reduce the optical loss associated with multiple diffracted beams. It is expected that an order-of-magnitude improvement in total coupling efficiency will be obtained with the asymmetric guide despite of the optical losses associated with both guided-wave absorption in the metal film and mode conversion.

3.2 Preliminary Experimental Results for Symmetric Waveguides

As discussed in previous technical reports (Ref. 2 and 4), there are optical losses at each grating associated with the occurrence of two beams for the single diffracted order allowed by the grating equation. A modulator holder has been

designed that allows all diffracted beams for the symmetric waveguide to be ovserved simultaneously and the distribution of diffracted energy to be determined.

Figure 8 summarizes the initial results of a study of a symmetric waveguide with grating couplers. Even though only a single guided mode was excited at the input grating, a total of six diffracted beams were observed at the output grating. Mode conversion that occurred along the 3 cm path between the gratings caused about 25 percent of the guided energy to couple from the dominant mode, tentatively identified as TE_2, into two lower-order modes. As a result, three beams corresponding to three distinct guided modes were observed above the output grating. Because of the symmetry of the waveguide, the same three modes were also partically coupled out of the bottom of the waveguide, as shown in Fig. 8. For the particular waveguide tested, the total energies in the two sets of beams were approximately equal. Similar results were obtained when the input coupling angle was changed and other guided modes were excited at the input grating.

The input coupling efficiency was determined to be 12 percent by observing the total power in the reflected and transmitted beams at the input both when the grating was properly oriented for maximum coupling and when the coupling was eliminated by slightly angular misalignment of the grating. The difference between the two values was taken as the power coupled into the guided mode.

The simultaneous existence of two sets of out-coupled beams containing a total of six beams clearly presents a loss for the waveguide modulator. Since only a single beam can be retained as useful output, about 60 percent of the out-coupled energy cannot be used. In addition, nearly 30 percent of the light appears to be lost from scattering and absorption in the waveguide. Even though the output grating is sufficiently long to couple out virtually all the guided energy, therefore, only about 3.5 percent of the input energy could be used despite an effective total coupling efficiency of 12 percent (input coupling efficiency of 12 percent times an effective output coupling efficiency of 100 percent). These results obtained with a laboratory waveguide, might be somewhat degraded if the symmetric waveguide were to be clamped into a metallic microwave ridge guide in which the waveguide boundary is perturbed by irregular metal-dielectric interfaces.

The performance of the grating in Fig. 8 has not been fully optimized because the input beam is not the correct size for aperture matching. Experiments now in progress will determine the proper beam size for aperture matching. In addition, the dependences of both waveguide losses and mode conversion on the order of TE mode excited at the input will be determined. This information will indicate the choice of input coupling angle for maximum useful coupling. As a result of such optimization, the input coupling efficiency will be increased. Useful total coupling efficiencies as high as 30 percent are expected with the symmetric waveguide. The power loss from multiple output beams will not be effected by this optimization, however.

FIG. 8

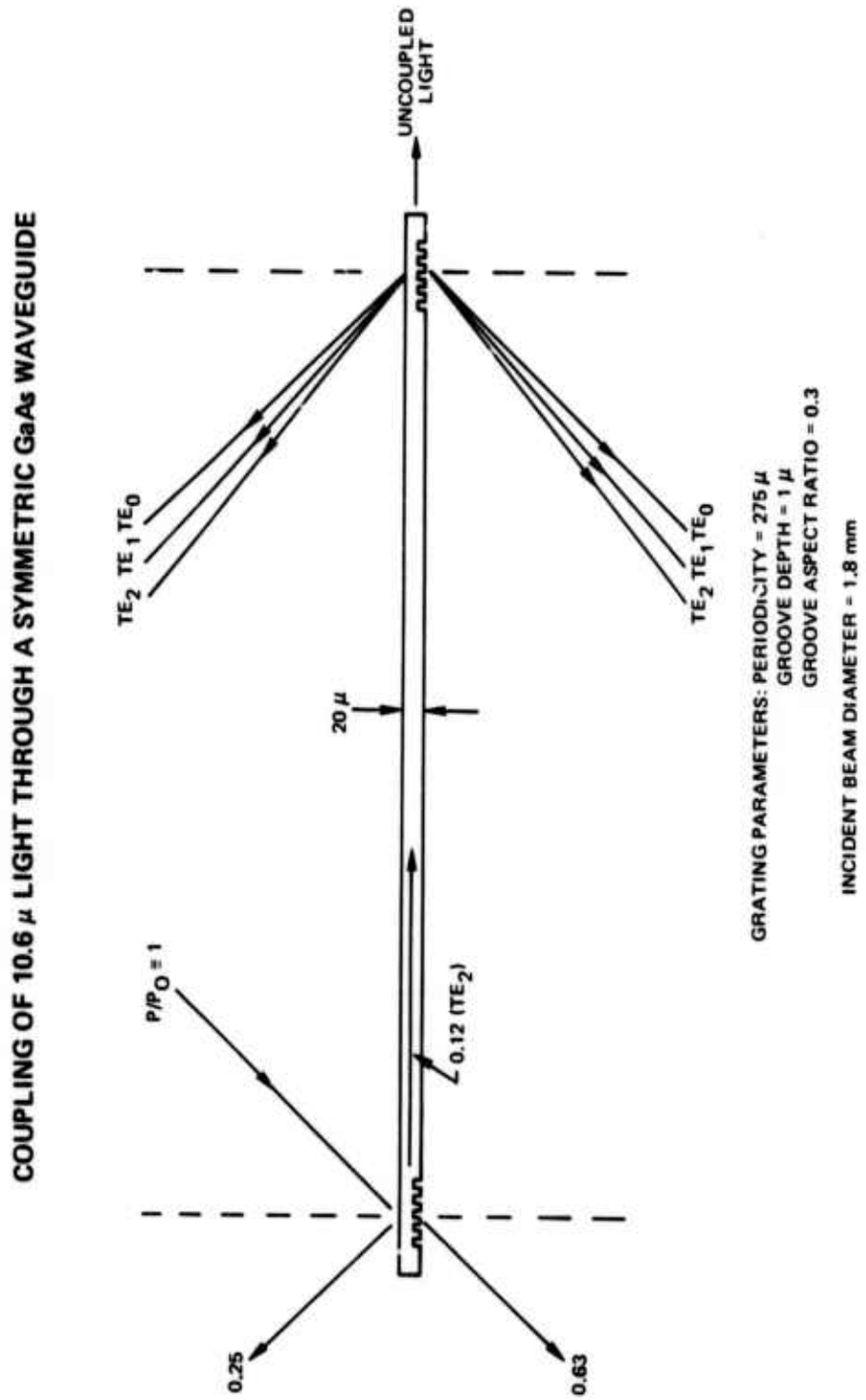

3-2a

N09-95-1

Metalizing one side of the wafer could substantially increase the useful coupling efficiency. Because the metal film will produce a uniform metal-dielectric interface, metal coating will tend to suppress mode conversion within the modulator. More important, it will prevent the development of both the transmitted beam and the lower set of out-coupled beams. With proper aperture matching, the transmitted energy can be redirected into the waveguide and the useful output greatly increased. In addition, if the metal is placed on the grating side, the grating will diffract more strongly, thereby allowing proper aperture matching to be achieved with smaller grating couplers.

During the next reporting period the coupling characteristics of metallized waveguides as well as the blazed gratings will be carefully studied. The characteristics of these couplers will be compared to those of uncoated symmetric waveguides having identical coupler geometries.

4.0 MICROWAVE STUDIES OF WAVEGUIDE MODULATORS

4.1 Introduction

The microwave work has been continued in the 16 GHz frequency range during this period with a detailed investigation of both the standing-wave and the traveling-wave structures. The standing wave (resonant) structure was used for the modulation experiments while the traveling wave structure was used for preliminary evaluation leading to the development of the desired broadband microwave modulation. In both cases the modulator configurations consisted of a mini-gap ridge waveguide structures with cross-sections for the interaction region (containing the thin dielectric slab) 1.0 millimeters wide and 25 microns high.

The two basic modulator structures are depicted in Fig. 9. The input and the output microwave lines are oriented 90° with respect to the optical path so that the rf input connections will not interfer with the optical transmission path. These lines also serve as the impedance transformers required for broadband matching. For clarity the outer shields of the ridge waveguide, for both configurations, are not shown in this figure.

For efficient modulation, it is necessary that the microwave be synchronized with the optical wave passing through the modulator. As already discussed in a previous report (Ref. 2), a slow-wave structure is a convenient one to use in preliminary experiments because it is simple to construct. The synchronization technique is illustrated in Fig. 10. It is a plot of angular frequency (ω) versus electrical length (βL). In this figure, the slope of line that is drawn from any point on the curve to the origin is proportional to the phase velocity. Three curves are shown in Fig. 10, one of which is for the ridge structure under the assumption that a perfect synchronization is achieved. In this case the phase velocity is slightly lower than that for the microwave along the smooth ridge structure. Another curve represents the ridge waveguide with periodic discontinuities. The parameters of the discontinuities are selected such that the phase velocity of the microwave is reduced to obtain a reasonable match to that of the optical wave. The disadvantage of using periodic discontinuities is that it introduces cut-off frequency for the propagating wave. We have analyzed the problem of synchronization in detail and have established criteria for the required degree of synchronization. It is obvious from the curves of Fig. 10 that exact synchronization is not possible because of the difference in the shapes of these curves.

During this period we have also studied the broadband matching problem both theoretically and experimentally. Because of difficulties encountered with the modulator in its present form, considerations have been given to improve the modulator configuration in such a way that the performance of the modulator would be more reproducible.

MODULATOR CONFIGURATIONS

TRAVELING WAVE MODULATOR

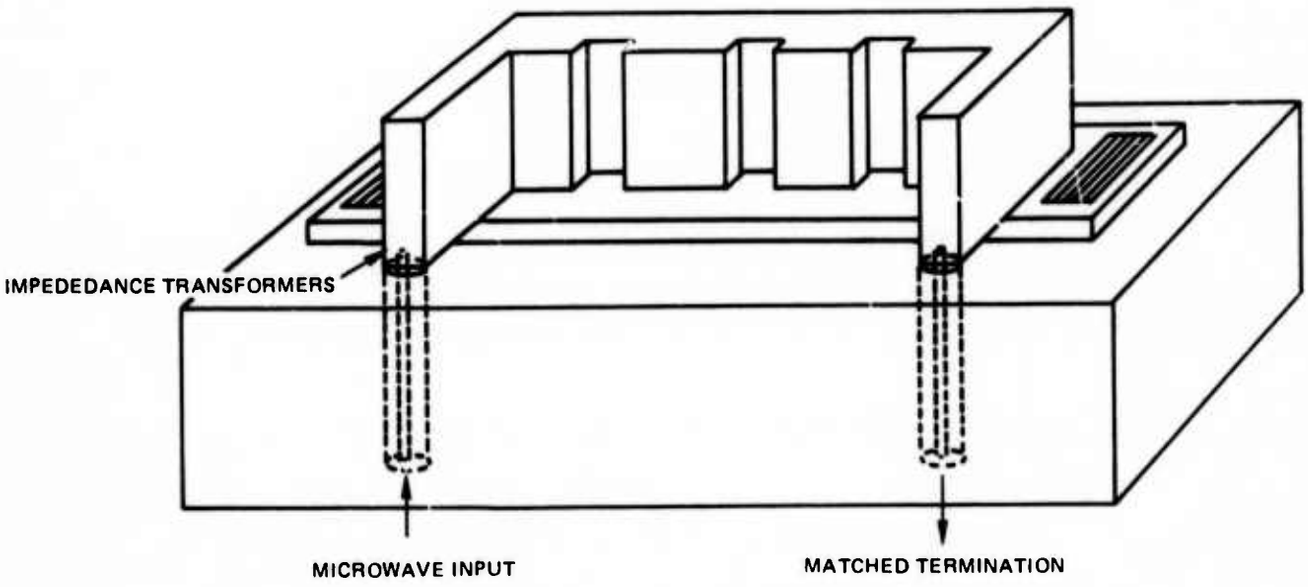

STANDING WAVE MODULATOR

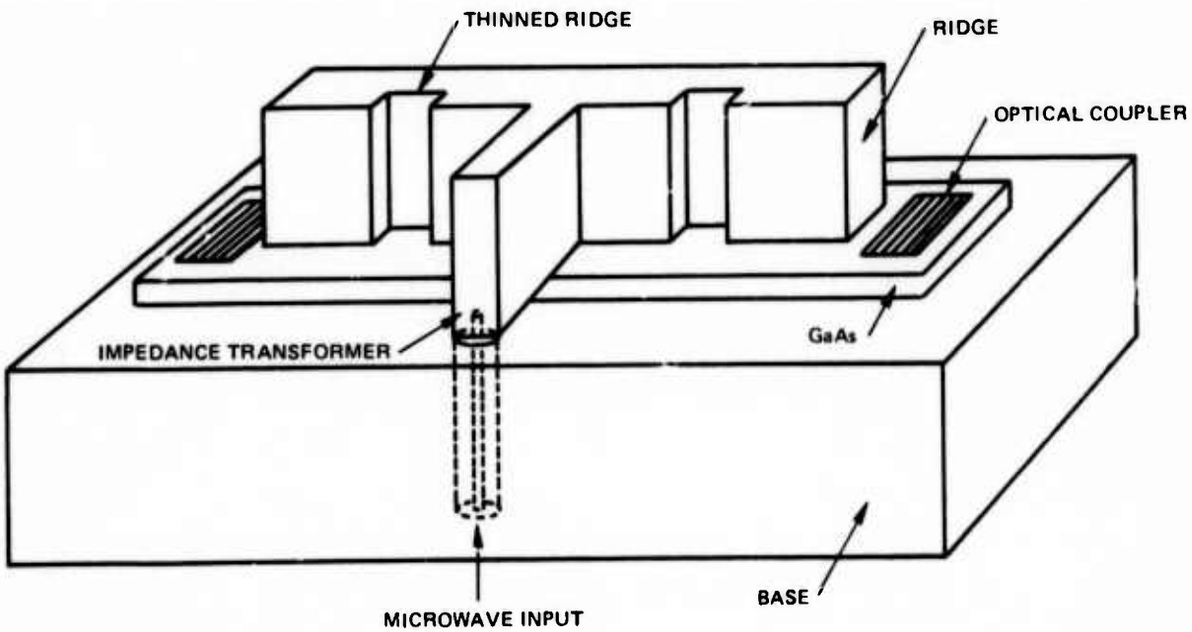

4-1a

FIG. 10

$\omega - \beta$ DIAGRAM FOR SLOW WAVES ON MODULATOR STRUCTURE

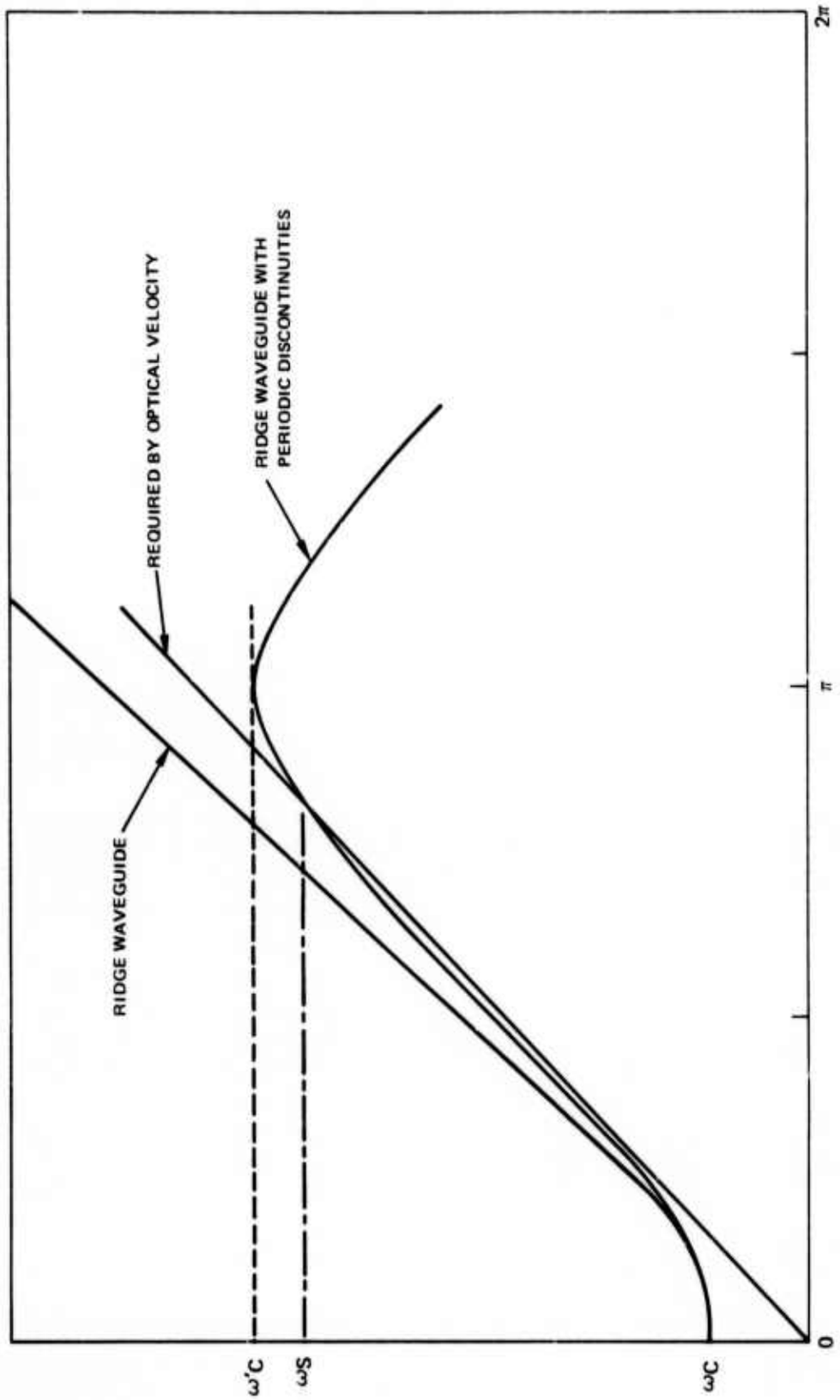

N09-75-4

4.2 Sychronization For The Ridge Waveguide

We now consider the problem of synchronization of the microwave and optical wave and attempt to establish a criterion for the degree of synchronization. The accumulated phase shift of the optical beam for interaction length L is given by the expression,

$$\Delta\phi = (\pi n^3 r_{41}/\lambda t)\int_0^L V_0 e^{-ax} \cos bx \, dx \qquad (3)$$

where n is the index of refraction
r_{41} is the electrooptic coefficient of GaAs
λ is the optical wavelength
t is the slab thickness
V_0 is the input synchronous voltage wave amplitude
a is the microwave attenuation constant
and $b=\beta_o-\beta_M$ is the difference of propagation constants of the optical guided wave and the microwave

The lack of synchronization is accounted for by the cosine term under the integral sign. The normalized phase shift, upon carring out the integration in Equation (3), is,

$$\frac{\Delta\phi}{\Delta\phi_o} = \frac{1}{(aL)^2 + (bL)^2}\left[aL(1-e^{-aL}\cos bL) + bLe^{-aL}\sin bL\right] \qquad (4)$$

It should be noted that for the case where the microwave attenuation factor is zero, the phase shift follows a (sin x)/x characteristic, as given by

$$\frac{\Delta\phi}{\Delta\phi_o} = \frac{\sin bL}{bL} \qquad (5)$$

The results for several values of aL are plotted in Fig. 11. An examination of these results indicates that a total difference in phase shift of about 60° for a given length, L, would be acceptable for this modulator. The degradation in the sideband power for this amount of phase difference would be approximately 50% (or 3dB). The mismatch in phase velocities for $aL < 0.1$ can be expressed as:

traveling wave $$\Delta\phi_T \simeq \frac{\pi}{\lambda} n^3 r_{41} L(PZ_o)^{1/2} S(bL) \qquad (6)$$

standing wave $$\Delta\phi_S \simeq \frac{\pi}{\lambda} n^3 r_{41} (PZ_o \frac{L}{a})^{1/2} S(bL) \qquad (7)$$

FIG. 11

EFFECT OF LACK OF SYNCHRONIZATION AND MICROWAVE ATTENUATION

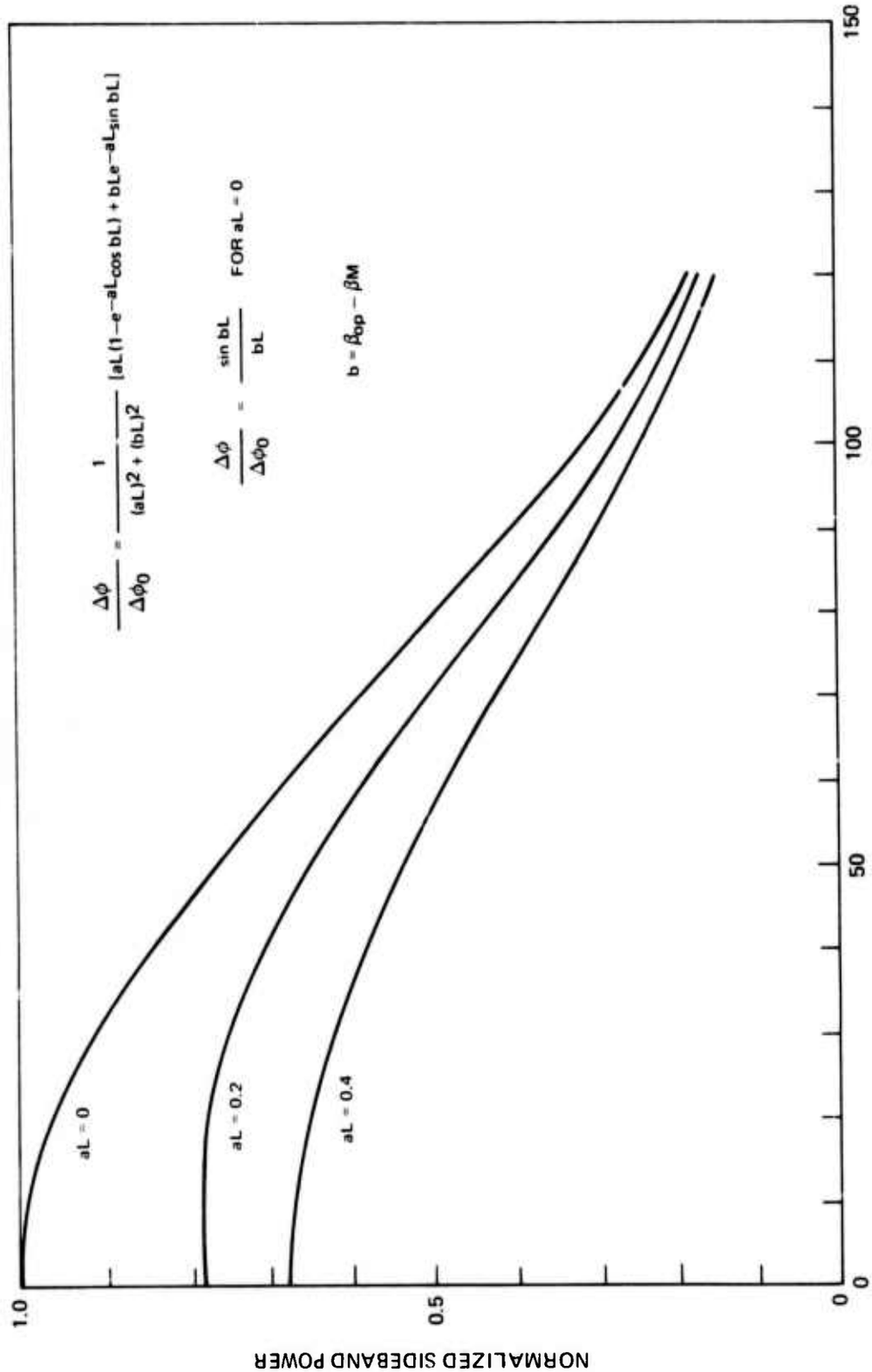

4.2a

where S(bL) is a degradation factor as a result of the velocity mismatch. From more exact expressions for Equations (6) and (7) we obtain that

$$\frac{\Delta\phi_S}{\Delta\phi_T} = (1-e^{-4aL})^{-1/2} \qquad (8)$$

It is noted that Equation (8) always gives a value larger than unity. This implies that the standing wave resonator will always give a larger phase shift; however, for a reasonably large attenuation factor, this ratio approaches unity.

The results on synchronization are summarized in Fig. 12. It shows the characteristics of a representative slow-wave transmission line both with and without the periodic discontinuities. Figure 12 also includes an ω-βL plot for the case where the microwaves are traveling at the optical velocity. The shaded area represents the region where the degree of mismatch in terms of electrical length reaches $\pm 60^{\circ}$. These curves were computed from an accurate computer model that included losses, and they show in detail the results of a properly designed slow-wave structure. Figure 12 also includes the calculated attenuation. These results show how attenuation begins to increase rapidly as the β values approach the cut-off frequency. Synchronization has also resulted in an increase in the characteristic impedance for this particular modulator from 5 ohms to 6.5 ohms. In this model, the periodic discontinuities in the transmission line consisted of thirteen short high impedance sections. The approximate modulator length was three centimeters. These calculations show that synchronization can readily be achieved over more than the desired bandwidth of 1.5 GHz. It is also noted that the parameters of this slow-wave structure are not optimum for operation at 16 GHz. A structure with a higher cut-off frequency would be more desirable in order to reduce attenuation.

A second set of calculated characteristic curves for a 12 section slow-wave structure are given in Fig. 13. The axes have been interchanged and the values for βL now correspond to the phase shift per section; but, the calculated attenuation corresponds to the full 12 sections. These curves show the relationship between the cut-off frequency and the value of characteristic impedance in the periodic discontinuities. In these calculations the frequency range was extended to show the saturation effect on the phase shift per section. The characteristic impedance of a section of the periodic structure was determined by interative computer calculations, in which the equal output load and generator impedances were varied together until the calculated input impedance best coincided with the load resistance over the broadest band of frequencies. This value of load resistance was taken as Z_o.

The theoretical calculations were confirmed by experiments with a 30 micron thick GaAs sample in which the wave slowing was accomplished by removing material from the side wall of the ridge as was shown in Fig. 9, to form the desired periodic structure. A plot of the measured phase shift per section as a function of frequency, is shown in Fig. 14. The data points were obtained by measuring resonant frequencies

FIG. 12

THEORETICAL CHARACTERISTICS OF A REPRESENTATIVE SLOW WAVE LINE

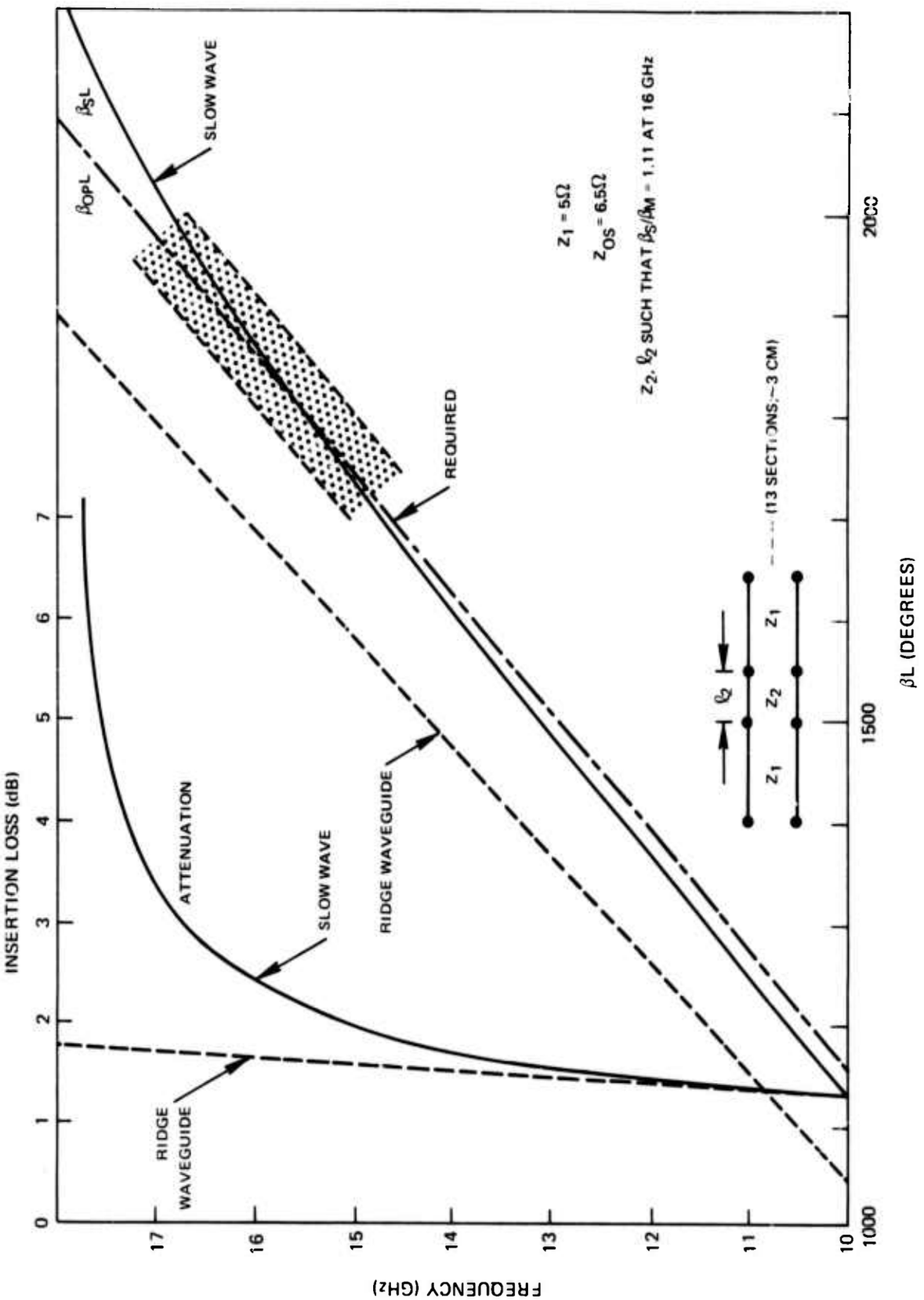

4-3a

N09-75-2

FIG. 13

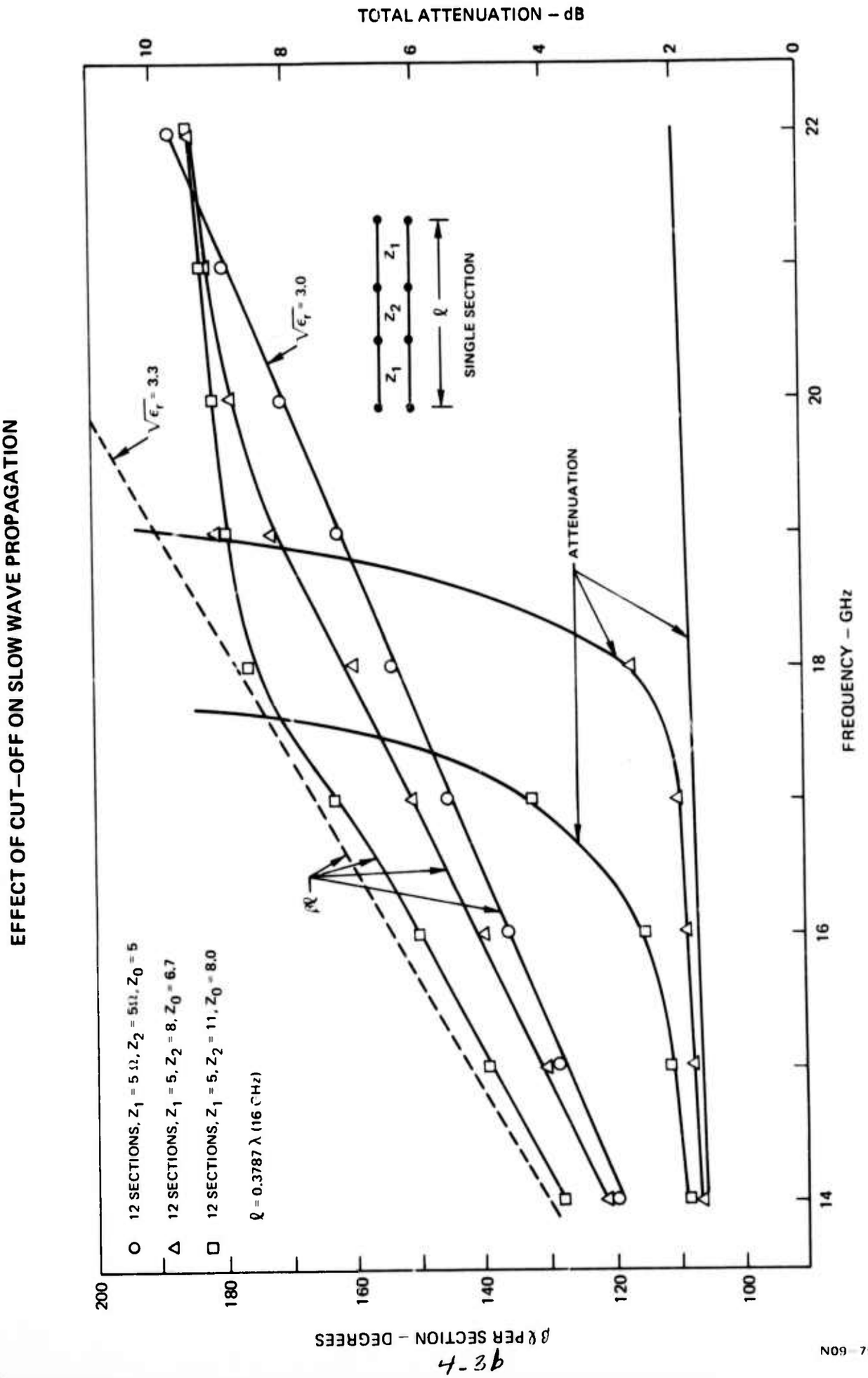
EFFECT OF CUT–OFF ON SLOW WAVE PROPAGATION
TOTAL ATTENUATION – dB
10
8
6
4
2
0
22
20
18
16
14
FREQUENCY – GHz
ATTENUATION
$\sqrt{\epsilon_r} = 3.3$
$\sqrt{\epsilon_r} = 3.0$
Z_1
Z_2
Z_1
ℓ
SINGLE SECTION
$\beta\ell$
O 12 SECTIONS, $Z_1 = 5\ \Omega$, $Z_2 = 5\Omega$, $Z_0 = 5$
Δ 12 SECTIONS, $Z_1 = 5$, $Z_2 = 8$, $Z_0 = 6.7$
□ 12 SECTIONS, $Z_1 = 5$, $Z_2 = 11$, $Z_0 = 8.0$
$\ell = 0.3787\ \lambda$ (16 GHz)
200
180
160
140
120
100
$\beta\ell$ PER SECTION – DEGREES
4-36
N09-75-7

FIG. 14

EXPERIMENTAL RESULTS WITH A SLOW WAVE ON RIDGE WAVEGUIDE

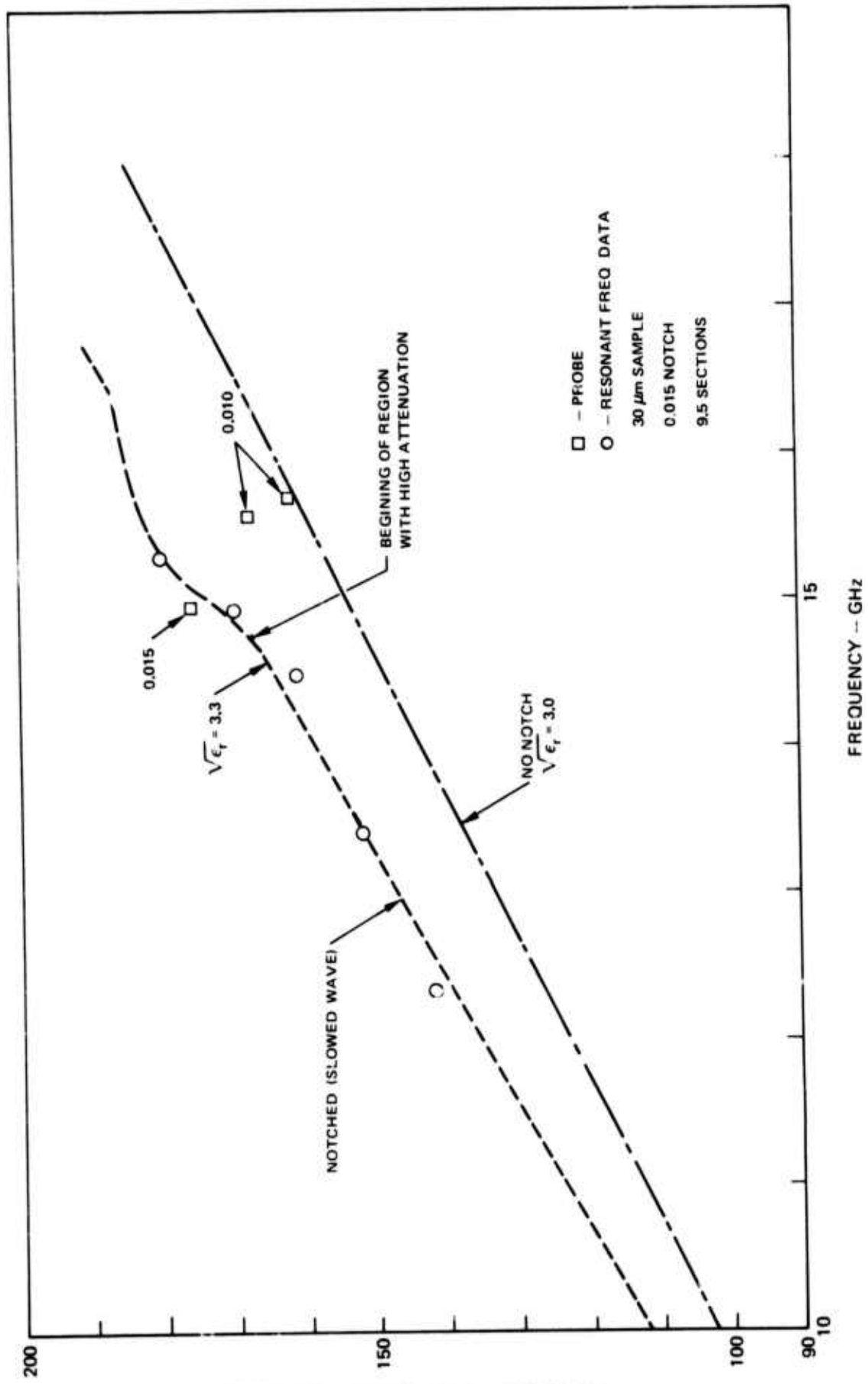

4-3c

of the structure. The length of transmission line was long enough so that a number of resonances could occur. At each resonant frequency the electrical length of line would be a multiple of 180 degrees. The thinned sections had 15 mils of material removed. Figure 14 also includes a curve with a slope corresponding to the nominal value of phase velocity for the ridge waveguide without the periodic discontinuities. Figure 14 includes, as well, data points which were experimentally determined by moving a small perturbing metallic probe along the edge of the ridge structure so that the half wavelength distances could be determined directly. The input impedance of the ridge structure will go through one complete period of variations for each half wavelength. This structure gave the desired slow-wave velocity but the cutoff frequency is too low for operation at 16 GHz.

It is very likely that the structure probably can not be made accurate enough to accomplish the desired degree of synchronization. Therefore, some fine-tuning technique will be required in order to optimize the phase velocity under experimental conditions. Such adjustment for synchronous conditions have been used for a bulk microwave modulator (Ref. 9).

4.3 Broadband Impedance Matching

One of the important requirements for the development of a traveling-wave microwave modulator is to achieve the broadest bandwidth at a reasonable microwave power level. With a computer model, we have calculated the frequency response of the impedance matched slow-wave structure identical to that discussed above (Fig. 13), including the effect of attenuation. The results are shown in Fig. 15. The main result is that an insertion loss of approximately 2dB can be obtained over a bandwidth of 2 GHz with the parameters indicated. Within this bandwidth the insertion loss with the matching transformers approaches that of the slow-wave structure without the matching transformers. This is a significant result because it shows that a single step transformer at both input and output ends should be sufficient to achieve the required bandwidth. If this were not the case, additional transformer steps would be required in order to get the desired bandwith. An example of experimental broadband matching is shown in Fig. 16 for a 42 micron thick sample. The input and output transformer sections were adjusted empirically to obtain an input VSWR less than 1.5 in the 15 to 17 GHz frequency range, as shown in Fig. 16. Although similar impedance matching was not done for a periodic structure, these results are indicative that broadband matching should be obtainable with the desired modulator structure.

4.4 High Power Testing

It is anticipated that this modulator might be used at power levels up to 100 watts for the generation of highest sideband power. In the case of the resonant

THEORETICAL CHARACTERISTICS OF A REPRESENTATIVE SLOW WAVE LINE

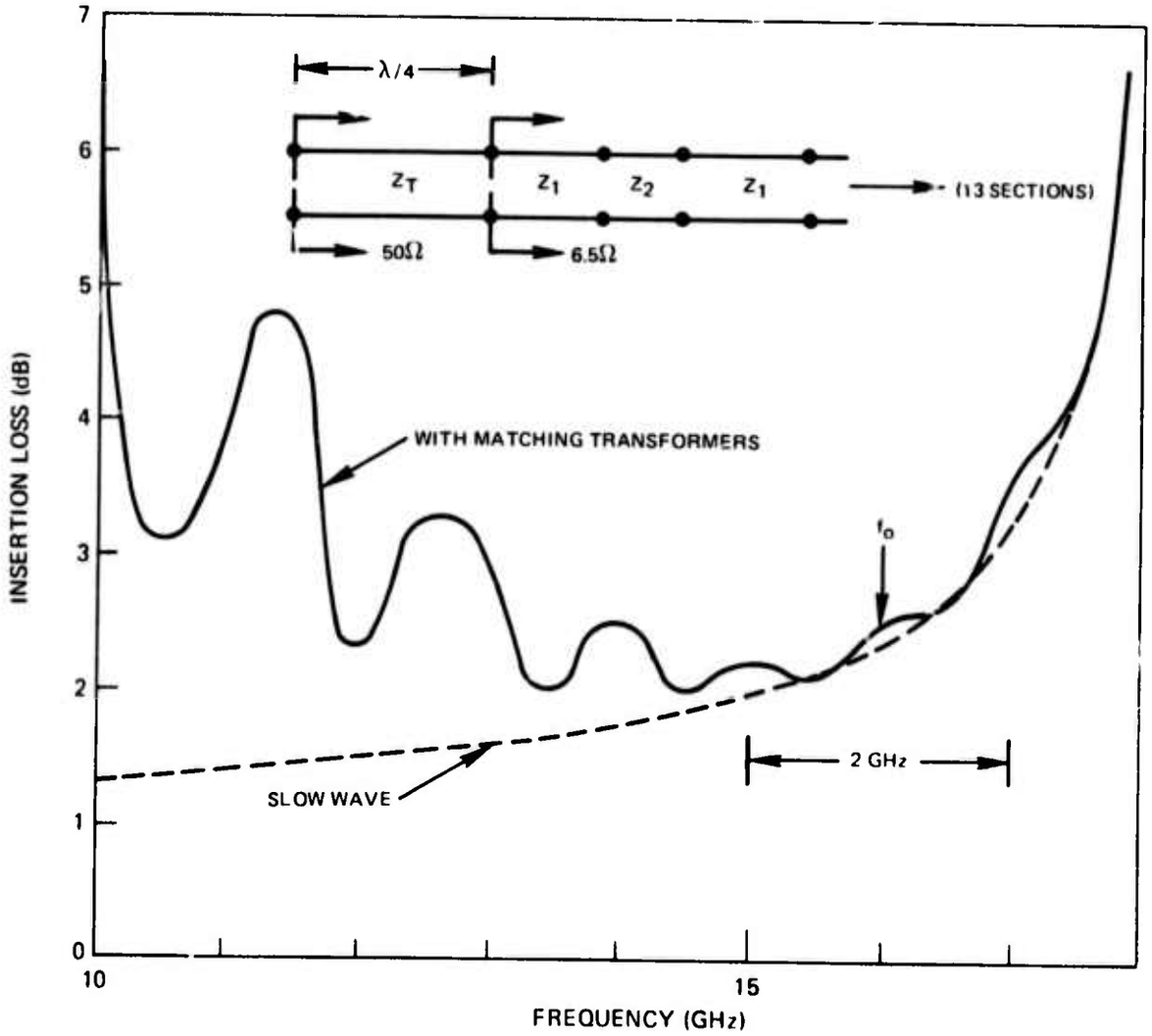

4.4a

EXPERIMENTAL BRAOD–BAND MATCHING

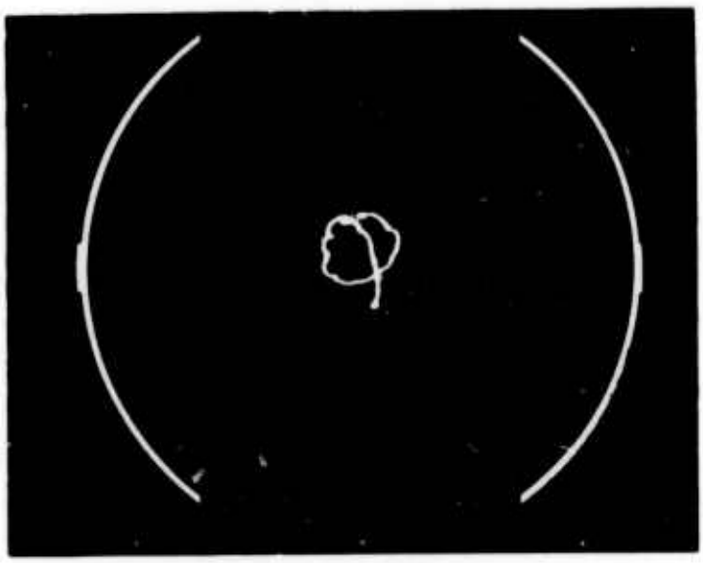

15–17 GHz (VSWR<1.5)

a) INPUT REFLECTION COEFFICIENT

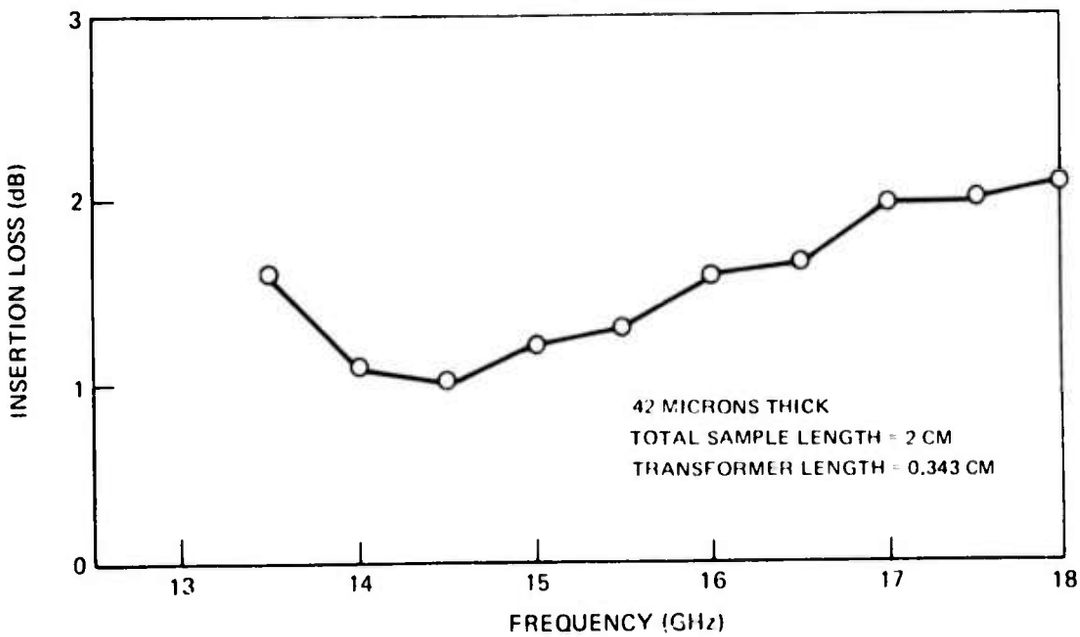

b) INSERTION LOSS

4-4b

modulator the entire 100 watts would be dissipated internally whereas in the case of the traveling wave modulator, a substantial portion of the 100 watts would be delivered to an external load. In anticipation of operating at these power levels, water channels for heat removal were provided in the copper blocks which formed the ridge waveguide structure. Since a large fraction of the power loss is in the conductors the actual heat dissipation in GaAs is very small. In an experiment, a two centimeter long resonant structure has been tested under cw conditions at power levels up to 100 watts. It was found that this modulator structure could handle 100 watts microwave power. However, without water cooling or without the proper attention to heat removal, considerable damage to the modulator was observed. Since we found that some of the standard commercial coaxial connectors are not suitable for this application, special consideration must be given to the modulator input structure design. The design will provide additional cooling of the input lines and bring the microwave power directly to the thin-slab modulator through a rectangular waveguide.

4.5 Modulator Reliability

The ridge waveguide modulator structures used in our work so far have produced a significant amount of useful information; however, the structural design requires modifications and improvement. The major difficulty encountered in using these structures is the lack of reproducibility of the microwave characteristics. During this reporting period we have explored techniques for improving this aspect of the modulator. One very significant approach, which has been discussed in some detail in Section 2, is the use of metalized layers deposited directly onto the GaAs slab surfaces. This would include both the ground plane and the region of the ridge section (see Fig. 8). In this way, a more reproducible transmission line in terms of its characteristic impedance and slow-wave characteristics may be obtained. In order to properly evaluate the metalization technique, a 10 mil sample of Gallium Arsenide was selected as the study vehicle. With the exception of thickness, samples have been prepared with the same dimensions for the metalization as those used for the actual modulator. Eventually work will be done with the 1 mil samples. The reason for choosing thicker (10 mil) samples is because that more accurate measurements can be made with these thicker samples in determining the effect of the metalization.

Metalized samples have been fabricated and evaluated both in the ridge waveguide structure and in microstrip configuration. The microstrip structure provides an easier proceedure for evaluating losses of the transmission line. In all cases the transmission line parameters were determined by resonant techniques employing both open circuits and a 50 ohm terminations at the end of the sample lines. In addition, with the microstrip structure, it was also possible to use a time-domain-reflectometer to determine directly the characteristic impedance of the line as well as any unusual perturbation at the interface between the input line and the modulator transmission line. The ridge waveguide, on the other hand, has a low-frequency cut-off and therefore the domain reflectometer can not be used readily.

An approximate model was used to estimate the characteristic impedance of the microstrip line. The model included the effect of fringing fields, which extend beyond the metalization by using an effective conductor width equal to the actual width plus the sample thickness. The calculated characteristic impedance of the 10 mil thick line was 23 ohms as compared to a value of 20 ohms measured directly with the time-domain-reflectometer. By extrapolating these results for waveguides having a thickness of 1 mil, a characteristic impedance of approximately 2.8 ohms is expected. This value is smaller by approximately a factor of two from the values measured earlier (Ref. 2) for the ridge structure where no direct metalization was used on the Gallium Arsenide. The difference is not surprising since the metal conductors are now in a more intimate contact with the GaAs slab. This suggests that there should be a higher degree of reproducibility also. From resonant frequency measurements and the known values of Z_o, the losses in the 10 mil ridge waveguide section were determined to be approximately 0.14dB per centimeter as compared to a value of 0.11dB per centimeter calculated from the simple theoretical model. On the other hand, a value of 0.45dB per centimeter was measured for the same sample, mounted on the modulator base plate, but connected as a microstrip resonator. This result was somewhat unexpected. It turns out that the excessive loss was caused by a lossy connection from the coaxial input to the top conductor. When the same sample was remounted and used with a conventional microstrip launcher, the measured losses agreed, within experimental error, with the ridge waveguide measurements. Theoretically one would expect the attenuation for the 1 mil section to be approximately a factor of ten higher than measured values for the ten mil section. Some preliminary measurements made on a 1 mil metalized section in the ridge width waveguide yielded an attenuation of 0.7dB per centimeter. Eventhough, this was not an accurate measurement, it is clear that these losses in one mil section are close to the expected values. The determinations of the phase velocities in the metalized samples yielded values close to that expected for propagation in a homogeneous GaAs medium both for the filled ridge-waveguide and the GaAs microstrip configurations.

Work on the evaluation of the direct metalization with the aim of measuring more accurate loss characteristics will be continued. Techniques will be developed to further improve the metalization process so that the losses can further be reduced, and better reproducibility be established. Consideration will also be given to a new modulator structure design with provisions for fine-tuning of the phase velocity of propagation while the modulator is in operation so that small phase velocity changes can be made in order to achieve optimum modulation. The input and output of the small coaxial transmission lines will be redesigned to provide better cooling through more intimate contact with the water cooling system. These lines will be simplified and shortened so that they may be cooled more adequately and so that standard commercial coaxial connectors can be eliminated.

5.0 REFERENCES

1. P. K. Cheo and M. Gilden, Appl. Phys. Lett., 25, 272 (1974).

2. P. K. Cheo, M. Gilden, D. Fradin and R. Wagner, "Microwave Modulations of CO_2 Lasers in GaAs Thin-Film Optical Waveguide," UARL Semi-Annual Tech. Rep. N921513-6, Contr. No. N00014-73-C-0087, March, 1974.

3. T. Gilmartin, MIT Lincoln Laboratory (private communication).

4. P. K. Cheo, M. Gilden, J. F. Black and J. L. Swindal, "Ultra-Wideband Thin Film Modulator for CO_2 Lasers," UARL Semi-Annual Tech. Rep. M921513-4, Contr. No. N00014-73-C-0087, September, 1973.

5. P. K. Tien and R. Ulrich, J. Opt. Soc. Am. 50, 1325 (1970).

6. K. Ogawa, et. al., IEEE J. Quant. Electronics, QE-9, 29 (1973).

7. Hugh L. Garvin, "Ion Beam Sputtering for Thin Film Deposition and High-Precision Micromachining," 3rd Symposium on Thin Films By Sputtering.

8. K. Parker and H. Shah, "Residual Stresses In Electroless Nickel Plating," Plating, pp. 230, March 1971.

9. E. Bicknell, MIT Linclon Laboaratory (private communication).